

ADA 039906

9 (12)

## Optical Phase and Scintillation at AMOS

→ ~~Electronics Research Laboratory~~  
The Ivan A. Getting Laboratories  
The Aerospace Corporation  
El Segundo, Calif. 90245

15 April 1977

Interim Report

APPROVED FOR PUBLIC RELEASE;  
DISTRIBUTION UNLIMITED

Sponsored by  
DEFENSE ADVANCED RESEARCH PROJECTS AGENCY  
1400 Wilson Blvd.  
Arlington, Va. 22209

DARPA Order No. 2843

SPACE AND MISSILE SYSTEMS ORGANIZATION  
AIR FORCE SYSTEMS COMMAND  
Los Angeles Air Force Station  
P.O. Box 92960, Worldwide Postal Center  
Los Angeles, Calif. 90009



THE VIEWS AND CONCLUSIONS CONTAINED IN THIS DOCUMENT ARE THOSE  
OF THE AUTHORS AND SHOULD NOT BE INTERPRETED AS NECESSARILY  
REPRESENTING THE OFFICIAL POLICIES, EITHER EXPRESSED OR IMPLIED,  
OF THE DEFENSE ADVANCED RESEARCH PROJECTS AGENCY OR THE U.S.  
GOVERNMENT.

2 No.  
DDC FILE COPY

The interim report was submitted by The Aerospace Corporation, El Segundo, CA 90245, under Contract No. F04701-76-C-0077 with the Space and Missile Systems Organization, Deputy for Advanced Space Programs, P.O. Box 93960, Worldway Postal Center, Los Angeles, CA 90009. It was reviewed and approved for The Aerospace Corporation by A. H. Silver, Director, Electronics Research Laboratory. Lieutenant A. G. Fernandez, SAMSO/YAPT, was the project officer for Advanced Space Programs. This research was supported by the Defense Advanced Research Projects Agency of the Department of Defense.

This report has been reviewed by the Information Office (OI) and is releasable to the National Technical Information Service (NTIS). At NTIS, it will be available to the general public, including foreign nations.

This technical report has been reviewed and is approved for publication.

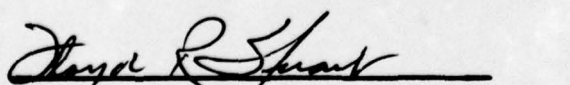


ARTURO G. FERNANDEZ, Lt, USAF  
Project Officer



ROBERT W. LINDEMUTH, Lt Col, USAF  
Chief, Technology Plans Division

FOR THE COMMANDER

  
Floyd R. Stuart, Colonel, USAF  
Deputy for Advanced Space Programs

## UNCLASSIFIED

SECURITY CLASSIFICATION OF THIS PAGE (When Data Entered)

REPORT DOCUMENTATION PAGE		READ INSTRUCTIONS BEFORE COMPLETING FORM
1. REPORT NUMBER SAMSO-TR-77-59	2. GOVT ACCESSION NO.	3. RECIPIENT'S CATALOG NUMBER
4. TITLE (and subtitle) OPTICAL PHASE AND SCINTILLATION AT AMOS		5. TYPE OF REPORT & PERIOD COVERED Interim report
6. AUTHOR(s) Hal T. Yura		7. PERFORMING ORG. REPORT NUMBER TR-0077(2756)-1
8. CONTRACT OR GRANT NUMBER(s) F04701-76-C-0077		9. PERFORMING ORGANIZATION NAME AND ADDRESS The Aerospace Corporation El Segundo, Calif. 90245
10. CONTROLLING OFFICE NAME AND ADDRESS Defense Advanced Research Projects Agency 1400 Wilson Blvd. Arlington, Va. 22209		11. PROGRAM/ELEMENT/PROJECT, TASK AREA & WORK UNIT NUMBERS DARPA order 2843
12. REPORT DATE 15 Apr 77		13. NUMBER OF PAGES 23
14. MONITORING AGENCY NAME & ADDRESS (if different from Controlling Office) Space and Missile System Division Air Force Systems Command Los Angeles, Calif. 90009		15. SECURITY CLASS. (of this report) Unclassified
16. DISTRIBUTION STATEMENT (of this Report) Approved for public release; distribution unlimited		
17. DISTRIBUTION STATEMENT (of the abstract entered in Block 20, if different from Report)		
18. SUPPLEMENTARY NOTES		
19. KEY WORDS (Continue on reverse side if necessary and identify by block number) Turbulence Scintillation Phase Coherence Atmospheric Optics		
20. ABSTRACT (Continue on reverse side if necessary and identify by block number) We present calculations of both the log-amplitude variance and phase coherence diameter for stellar sources at AMOS and compare our results to the measured value of the corresponding quantities, as performed by AVCO on the nights of November 17, 18, and 21, 1975. Our calculations are based, in part, on R. E. Hufnagel's recent model of atmospheric turbulence. We find fairly good agreement with the scintillation data, the agreement with the phase data being only fair to good. Although the results presented here are encouraging, more data		

UNCLASSIFIED

SECURITY CLASSIFICATION OF THIS PAGE(When Data Entered)

19. KEY WORDS (Continued)

20. ABSTRACT (Continued)

comparison is needed before the validity for general use at AMOS of the turbulence model used here can be established.

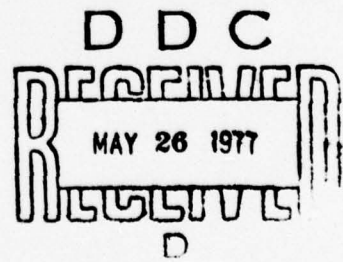
UNCLASSIFIED

SECURITY CLASSIFICATION OF THIS PAGE(When Data Entered)

## PREFACE

We acknowledge with appreciation D. Chang of The Aerospace Corporation for performing the numerical calculations, M. Miller of AVCO who supplied us with the relevant experimental data, and Maj. J. Madura of SAMSO who provided us with wind speed data.

PRESSESSION for	
VS	White Section <input checked="" type="checkbox"/>
	Buff Section <input type="checkbox"/>
SPECIFIED	
SPECIFICATION	
STOCK/AVAILABILITY	
MAIL AND/OR SPECIAL	
A	



CONTENTS

PREFACE .....	1
I. INTRODUCTION .....	5
II. ATMOSPHERIC TURBULENCE PROFILE .....	7
III. IRRADIANCE STATISTICS, <i>and</i> .....	9
IV. PHASE COHERENCE STATISTICS .....	15
REFERENCES .....	23

PRECEDING PAGE BLANK-NOT FILMED

## FIGURES

1.	Calculated value of the log-amplitude variance at a point as a function of the rms wind speed .....	12
2a	Turbulence Profile vs Height Above the Observatory - 17 November 1975 .....	17
2b.	Same as Figure 2b for 18 November 1975 .....	17
2c.	Same as Figure 2b for 21 November 1975 .....	18
3.	The phase coherence diameter $\lambda = 0.633 \mu\text{m}$ as function of rms wind speed .....	19

## TABLES

1.	Log-Amplitude Data Comparison ( $D = 35.6 \text{ cm}$ , $A \approx 0.019$ ) .....	14
2.	$r_o$ Data Comparison, $\lambda = 0.63 \mu\text{m}$ .....	20

## I. INTRODUCTION

The purpose of this report is to seek to determine if any correlation exists between measured values of both stellar scintillation and phase coherence and the corresponding values predicted from a recent model of the atmospheric turbulence profile. Specifically, we employ here Hufnagel's<sup>(1)</sup> recent model of the index structure constant profile  $C_n^2(h,V)$ , where  $h$  is the altitude above mean sea level and  $V$  is a root mean square wind speed (defined below) to calculate both the variance and covariance of the log-amplitude and phase coherence diameter  $r_o$  of an optical wave due to a stellar source. We then compare these quantities to the corresponding quantities as measured by AVCO and AMOS during November 1975.

We first discuss Hufnagel's recent model of  $C_n^2$  and present expressions for the appropriate wave statistical quantities. Using measured values of the wind speed parameter  $V$  for the appropriate dates of the experiment, we then proceed in Section IV to calculate the normalized log-amplitude variance and compare with the corresponding values, as measured by AVCO. For the three experimental dates considered, fairly good agreement is obtained.

In the design and deployment of the AMOS compensated imaging system, it is necessary to have knowledge of the statistical characterization of the phase coherence diameter of the atmosphere  $r_o$  of an optical stellar source. In Section IV we present the results of our calculation of  $r_o$  and compare with AVCO's experimental results. The present calculation of  $r_o$  is based on Hufnagel's recent model of  $C_n^2$  together with a low altitude  $C_n^2$  model (i.e., 0-3 km above the AMOS site) abstracted from the experimental results of Bufton<sup>(2)</sup> and Koprov and Tsvang<sup>(3)</sup>. Our calculated values of  $r_o$  are a little larger than AVCO's measured average values, although not as large as AVCO's value of  $r_o$  as calculated on the basis of measured turbulence profiles.

Although the present results are encouraging, more comparison with experimental data is needed before the validity of the turbulence model used here can be established. However, at this point we are cautiously optimistic.

## II. ATMOSPHERIC TURBULENCE PROFILE

Recently R. E. Hufnagel<sup>(1)</sup> presented an empirical model for the altitude profile of the index structure function  $C_n^2$ . In its full generality, the random turbulence version of the Hufnagel turbulence model has the form (in units of  $m^{-2/3}$ )

$$C_n^2(h) = 5.98 \times 10^{-23} (V/27)^2 h^{10} e^{-h} + 10^{-16} \times e^{-h/1.5} \exp[r(h,t)], \quad h > 3 \text{ km} \quad (1)$$

where  $h$  is in kilometers above mean sea level,  $V$  is the root mean square wind speed in meters/sec in the 5 to 20 km altitude range, i.e.,

$$V = \left[ \frac{1}{15 \text{ km}} \int_{5 \text{ km}}^{20 \text{ km}} v^2(h) dh \right]^{1/2}, \quad (2)$$

where  $v(h)$  is the wind speed profile in m/sec. The quantity  $r(h,t)$  is a gaussian random variable which depends on altitude and time. As defined by Hufnagel,  $r$  has zero mean and a correlation function given by

$$\langle r(h + h', t + \tau) r(h, t) \rangle = A(10h') \exp(-\tau/300) + A(h'/2) \exp(-\tau/4800) \quad (3)$$

where  $t$  is time measured in seconds and the function  $A$  is given by

$$\begin{aligned} A(x) &= 1 - |x|, & |x| &\leq 1 \\ &= 0 & |x| &> 1 \end{aligned} \quad (4)$$

In some cases it may be more convenient computationally to use an exponential decay function, i.e.,  $A(x) = \exp(-|x|)$ .

As is discussed below, the available data does not warrant the use of the full random model of  $C_n^2$ . Accordingly, we employ the non-random model, obtained by taking the ensemble average of Eq.(1). We obtain ( $\langle e^r \rangle = e \cong 2.72$ )

PRECEDING PAGE BLANK-NOT FILMED

$$C_n^2(h, V) = 5.98 \times 10^{-23} (V/27)^2 h^{10} e^{-h} + 2.72 \times 10^{-16} e^{-h/1.5} \quad (5)$$

where  $V$  is given by Eq. (2). As discussed by Hufnagel<sup>(1)</sup>,  $V$  appears to be normally distributed about some average value. For example, for the state of Maryland,  $V$  appears to be normally distributed with an average value of 27 m/sec and a standard deviation of 9 m/sec. Below we use the value of  $V$  obtained from the wind speed profiles for the dates of the measurements, as supplied by the Air Weather Service.

Strictly speaking, Eq. (1) or (5) is valid for  $h \gtrsim 3$  km. Since the measurements we performed at AMOS, i.e., at an altitude of 3 km, Eq. (5) will suffice for the present analysis. However, for completeness we present a model developed from the empirical data of Koprov and Tsvang<sup>(3)</sup>, and J. Bufton<sup>(2)</sup> for the value of  $C_n^2$  at altitudes below 3 km:

$$C_n^2 = \begin{cases} 7.0 \times 10^{-14} h^{-4/3} & , \quad 10 \text{ m} < h < 100 \text{ m} \\ 1.5 \times 10^{-16} & , \quad 100 \text{ m} < h < 500 \text{ m} \\ 1.5 \times 10^{-16} - 1.125 \times 10^{-16} \left( \frac{h - 500}{500} \right) & , \quad 500 \text{ m} < h < 1000 \text{ m} \\ 3.75 \times 10^{-17} + 7.95 \times 10^{-17} \left( \frac{h - 1000}{1000} \right) & , \quad 1000 \text{ m} < h < 2000 \text{ m} \\ 1.17 \times 10^{-16} - 5.85 \times 10^{-17} \left( \frac{h - 2000}{2000} \right) & , \quad 2000 \text{ m} < h < 3000 \text{ m} \end{cases} \quad (6)$$

The model presented above is simple in many respects. It does not explicitly account for possible high turbulence peaks generated at frontal interfaces or sharp inversion layers. And, conceivably the numerical coefficients in model should be different over mountainous terrain. Nevertheless, it does seem to yield reasonable agreement with most of the observed stellar scintillation measurements taken in the past. The appeal of the model lies in the fact that there is only one parameter, the root mean square wind speed  $V$ , which characterizes the altitude dependence of  $C_n^2$ . This parameter is readily available for many experimental sites

and in particular it is available for AMOS. Finally, we note that it is expected that the largest variability of  $C_n^2$  is obtained near the ground, the high altitude turbulence being insensitive to effects of local terrain. As is discussed below, the effects of low altitude turbulence have little effect in producing scintillation. However, both low and high altitude turbulence are important in producing optical phase distortions.

### III. IRRADIANCE STATISTICS

In all cases considered here we are in the regime of weak optical scintillation; that is, we are in unsaturated regime of scintillation where the results of the Rytov approximation apply. The regime of weak scintillation is such that the normalized variance of log-amplitude,  $\sigma_I^2$ , is much less than unity. In this regime it is known<sup>(4)</sup> that the probability distribution of irradiance is log-normal (i.e., the natural logarithm of irradiance is normally distributed); that is, the probability density of irradiance is given by

$$P(i) = \frac{1}{\sqrt{2\pi} \ln(\sigma_I^2 + 1)} \left( \frac{1}{i} \right) \exp \left\{ - \frac{[\ln i + 1/2 \ln(\sigma_I^2 + 1)]^2}{2 \ln(\sigma_I^2 + 1)} \right\} \quad (7)$$

where

$$i = \frac{I}{\langle I \rangle} \quad , \quad (8)$$

$$\sigma_I^2 = \frac{\langle I^2 \rangle - \langle I \rangle^2}{\langle I \rangle^2} \quad , \quad (9)$$

$I$  is the instantaneous value of irradiance, and angular brackets denote the ensemble average. Thus,  $i$  is the instantaneous value of irradiance normalized by its mean, and  $\sigma_I^2$  is the normalized variance of irradiance. Examination of Eq. (7) reveals that the probability distribution of normalized irradiance is characterized by the single parameter  $\sigma_I^2$ , the normalized variance of irradiance.

For log-normal statistics, the normalized variance of irradiance for a point receiver is related to the variance of log-amplitude,  $\sigma_{\ell}^2$ , by the relation

$$\sigma_I^2 = \exp(4 \sigma_{\ell}^2) - 1$$

$$\approx 4 \sigma_{\ell}^2, \quad \sigma_{\ell}^2 \ll 1 \quad (10)$$

The introduction of the quantity  $\sigma_{\ell}^2$  as the basic parameter is operationally useful as this is the quantity that is usually measured. Thus for a given value of  $\sigma_{\ell}^2$ , the probability distribution of irradiance is determined completely.

We next present expressions that relate the log-amplitude statistics to the index structure profile, optical wavelength and propagation path. For weak scintillation conditions the log-amplitude correlation function for a point (i.e., stellar) source at infinity is given by<sup>(4)</sup>

$$B_A(\rho) = 4 \pi^2 k^2 \sec \theta^{11/6} \int_{h_1}^{\infty} C_n^2(h) dh \int_0^{\infty} J_0(K\rho) \Phi_n(K) \sin^2 \left[ \frac{K^2(h - h_1)}{2k} \right] K dK \quad (11)$$

where  $\rho$  is the separation in a plane transverse to the mean direction of propagation,  $\theta$  is the zenith angle,  $h_1$  is the altitude of the receiver,  $k$  is the optical wave number ( $= 2\pi/\lambda$ , where  $\lambda$  is the optical wavelength),  $J_0$  is the Bessel function of zero-order of the first kind,  $C_n^2(h)$  is the index structure profile, and  $\Phi_n(K) \simeq 0.033 K^{-11/3}$ .

The variance of log-amplitude is then given by

$$\sigma_{\ell}^2 = B_A(0) = 4 \pi^2 k^2 \sec \theta^{11/6} \int_{h_1}^{\infty} C_n^2(h) dh \int_0^{\infty} \Phi_n(K) \sin^2 \left[ \frac{K^2(h - h_1)}{2k} \right] K dK$$

$$\cong 0.563 k^{7/6} \sec \theta^{11/6} \int_{h_1}^{\infty} C_n^2(h) (h - h_1)^{5/6} dh \quad (12)$$

Examination of Eq. (12) reveals that owing to the  $h^{5/6}$  weighting function in the integrand, the value of  $\sigma_l^2$  is determined primarily from high altitude turbulence. Examination of Eqs. (5) and (12) reveals that for  $V \gtrsim 10$  m/sec the main contribution to  $\sigma_l^2$  is determined by the turbulence near the tropopause, i.e., at  $h \sim 10$  km. The integrand of Eq. (12) has a relative maximum for  $h = 10.83$  km, falling to one-half its maximum value at  $h \simeq 7.5$  and 15.5 km.

Equation (12) for  $\sigma_l^2$  pertains to the statistics of irradiance at a point. As the experiments at AMOS were performed with a finite size receiving aperture, it is necessary in our analysis to account for aperture smoothing. As is discussed below, the effects of aperture smoothing are determined not only by the log-amplitude variance  $\sigma_l^2$  but also by the shape of the correlation function  $B_A(\rho)$ . As such, it will also be necessary to compute the full correlation function  $B_A(\rho)$  for  $\rho \lesssim D$ , where  $D$  is the diameter of the receiving aperture ( $= 35.6$  cm for the AMOS experiments). This calculation is discussed in more detail later on in this section.

Upon substituting Eq. (5) into Eq. (12), we find that the log-amplitude variance at a point is given by

$$\begin{aligned}\sigma_l^2 &\approx \left[ 4.14 \times 10^{-2} \left( \frac{V}{27} \right)^2 + 2.48 \times 10^{-3} \right] \left[ \frac{0.5}{\lambda \text{ (micron)}} \right]^{7/6} \sec \theta^{11/6} \\ &= 4.14 \times 10^{-2} \left( \frac{V}{27} \right)^2 + 2.48 \times 10^{-3}, \text{ for } \lambda = 0.5 \text{ } \mu\text{m}, \theta = 0\end{aligned}\quad (13)$$

and is plotted in Fig. 1 as a function of  $V$  for the case  $\lambda = 0.5 \text{ } \mu\text{m}$  and  $\theta = 0$ . In order to compare with experiment, one must correct these values for the smoothing effect of the finite size collecting aperture.

As alluded to above, scintillation measurements performed with a finite sized collector include an aperture smoothing effect referred to in the literature as the aperture averaging effect. Thus, the log-amplitude variance obtained from a collector of diameter  $D$ ,  $\sigma_l^2(D)$ , is related to the corresponding point log-amplitude variance by

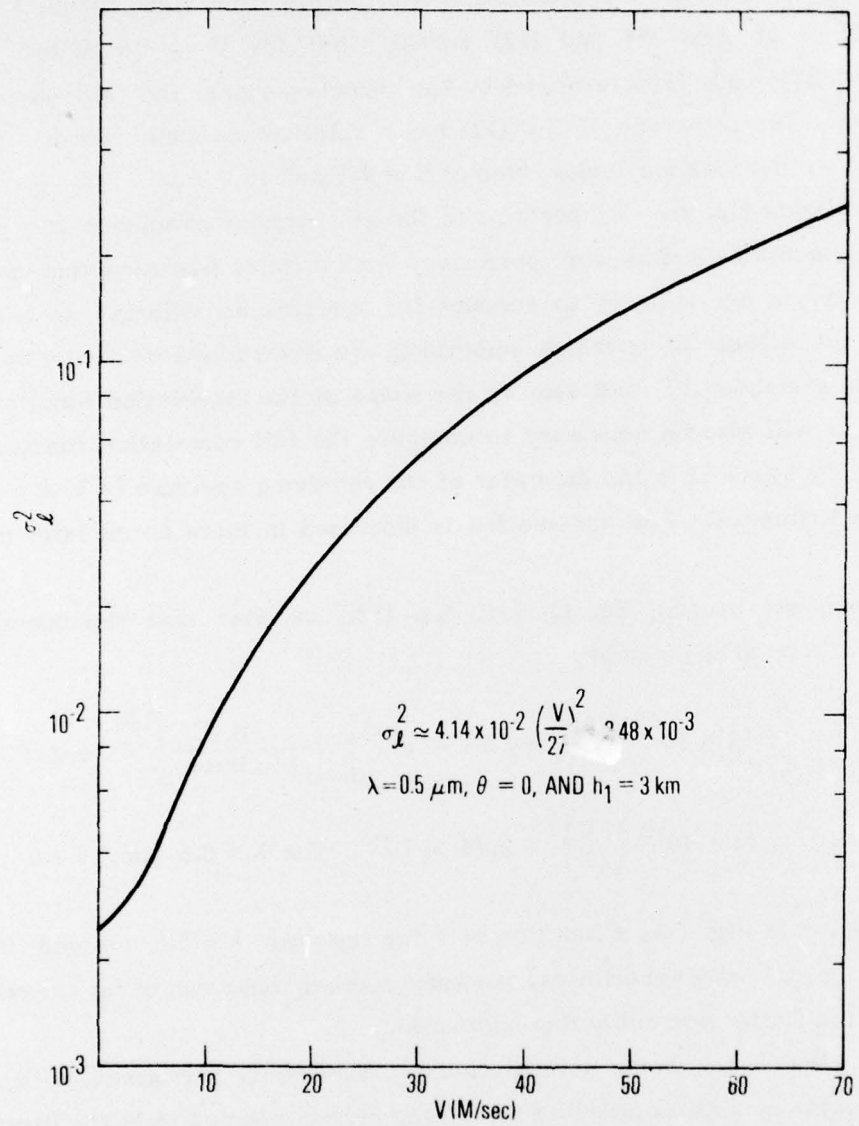


Fig. 1. Calculated value of the log-amplitude variance at a point as a function of the rms wind speed

$$\sigma_{\ell}^2(D) = A \sigma_{\ell}^2 \quad (14)$$

where the aperture averaging factor  $A (\leq 1)$  is given by<sup>(5)</sup> (we assume here that the collecting aperture is circular)

$$A = 8 \int_0^1 \frac{C_I(Dx)}{C_I(0)} M_L(x) x dx \quad (15)$$

where

$$M_L = \frac{2}{\pi} \left[ \cos^{-1} x - x \sqrt{1-x^2} \right], \quad 0 \leq x \leq 1$$

$$= 0, \quad x > 1 \quad (16)$$

$$C_I(\rho) = \exp \left[ 4 B_A(\rho) \right] - 1 \quad (17)$$

and  $B_A(\rho)$  is given by Eq. (11). Examination of Eqs. (11) and (17) reveal that the value of  $A$  depends on the characteristic correlation length of the log-amplitude correlation function  $p_{\ell}$ . For  $D \ll p_{\ell}$ ,  $A \approx 1$  and there is no aperture averaging effect, the receiver is essentially a point receiver. On the other hand, for  $D \gtrsim p_{\ell}$ , several "independent" fluctuations with differing signs are collected, and they partially compensate one another leading to a value of  $A < 1$ . For uniform turbulence condition the amplitude correlation length is of the order  $\sqrt{\lambda L}$ , where  $L$  is the path length and  $\lambda$  is the optical wavelength.

Examination of Eqs. (15) and (17) reveal that for  $B_A(0) = \sigma_{\ell}^2 < 1$  the value of  $A$  depends on the form of the normalized log-amplitude covariance function  $b_A(\rho) = B_A(\rho)/\sigma_{\ell}^2$  only. For values of  $V$  greater than about 10 m/sec the dominant contribution to  $b_A(\rho)$  results from the turbulence in the tropopause, i.e., the first term on the right-hand side of Eq. (1). In the experiments discussed below the value of  $V$  is in the 20 to 30 m/sec range. As a result, it can be shown for this case that  $b_A(\rho)$  is nearly a universal curve; that is,  $b_A(\rho)$  is independent of  $V$  for  $V \gtrsim 10$  m/sec. This implies that  $A$  is nearly independent of  $V$ . These results have been confirmed numerically for all values of  $V$  that were obtained in the AMOS experiments. We find that  $A \approx 0.019$  for the 14-inch diameter collector used at AMOS.

AVCO has performed scintillation measurements using a star sensor built by NOAA Environmental Research Laboratory. This instrument consists of a 35.6 cm Schmidt-Cassegrain telescope. When a stellar source is received through this system, measurements of the spatial frequency content of the atmospherically produced scintillation pattern are obtained. Details of the experimental apparatus and results obtained are reported elsewhere<sup>(6)</sup>. We have chosen three separate days to compare with. These days were chosen because the environmental profile  $C_n^2(h)$  was also measured independent of the optical measurements. Further details of the  $C_n^2$  measurements are also given in Ref. 6.

The nights chosen to compare our results to experiment are Nov. 17, 18 and 21, 1975. The experiments were generally run between 1900 to 2400 hours local time.

The wind speed data, obtained through Maj. John Madura of SAMSO, was taken at Hilo, Hawaii, at 2400 hours. Although Hilo, Hawaii, is about 100 miles from Maui, it is not expected that the values of  $V$  over Maui were significantly different than those over Hawaii, owing to the fact that the main contribution to  $V$  is at high altitude (5-15 km) and the terrain between the two islands is primarily open ocean. The value of  $V$  obtained are 21.3, 20.5, and 30.8 m/sec for Nov. 17, 18, and 21, respectively.

In Table 1 we have tabulated the values of  $\sigma_l^2$  obtained by AVCO at 0.5  $\mu\text{m}$  and the results of our calculations.

TABLE 1  
Log-Amplitude Data Comparison  
( $D = 35.6 \text{ cm}$ ,  $A \approx 0.019$ )

Date	$\sigma_l^2$ , AVCO		$\sigma_l^2$ , Aerospace Corp., $\theta = 0$	
	Range $\times 10^{-4}$	Average, $\times 10^{-4}$	Average, $\times 10^{-4}$	$V$ (m/sec)
Nov 17	2.79 - 18.20	7.92	5.37	21.3
Nov. 18	2.28 - 5.03	3.76	4.95	20.5
Nov 21	5.17 - 8.21	6.00	10.70	30.8

The AVCO data presented in the second column is a summary of twenty-minute log-amplitude variance measurements. The theoretical zenith angle dependence of  $(\sec \theta)^{11/6}$  was not removed by AVCO because "all data was collected on stars at low zenith angle (typically 10–20°, 30° maximum) and this effect should not be large." Our results are based on zenith propagation, i.e.,  $\theta = 0$ .

No attempt was made by AVCO to compare their optical scintillation results to the corresponding results obtained from the  $C_n^2$  profile that was measured on the dates of the experiments. Furthermore, an analysis of the variance of the  $\sigma_f^2$  was not performed, although enough data was recorded so that this information can be readily obtained. (Note: AVCO is in the process of doing this.)\*

Examination of Table 1 reveals that our calculated values of  $\sigma_f^2$  are in good agreement with AVCO's measured values; in two cases the calculated value is in the experimental range, while in the third case it is about 25% high. In view of the fact that some zenith angle biasing may be present [ $(\sec 30)^{11/6} = 1.3$ ] and the experiments were performed over several hours on each night, we feel that the results obtained here are encouraging enough to warrant further comparisons as more data is made available. We are in the process of doing this.

#### IV. PHASE COHERENCE STATISTICS

As is well known, the mutual coherence function (MCF) of the complex field due to a point source above the atmosphere is a central quantity in the evaluation of the AMOS compensated imaging system. Here we relate the coherence diameter  $r_o$  to the rms wind speed  $V$  and compare these results to the experimental values obtained by AVCO during Nov. 17, 18, and 21, 1975.

The MCF can be written as

$$M(r) = \exp \left[ -3.44 \left( \frac{r}{r_o} \right)^{5/3} \right] \quad (18)$$

where the coherence diameter  $r_o$  is given by

---

\* M. Miller, AVCO Everett Research Lab., private communication.

$$r_o \cong \left[ \frac{3.44}{1.45 k_v^2 \sec \theta \int_{h_i}^{\infty} C_n^2(h) dh} \right]^{3/5} \quad (19)$$

Examination of Eq. (19) reveals that in contrast to the case of scintillation, the coherence diameter depends both on low and high altitude turbulence (the weighting factor in the integrand of Eq. (19) being unity in the present case).

AVCO's measured turbulence profiles averaged over the complete data runs taken on 17, 18, and 21 Nov. 1975 are shown in Fig. 2. The lowest height (15 m) data points were obtained from the ground-based microthermal sensors. Data from 37 m to 2.5 km were provided by NOAA from a reduction of their (nighttime) airborne microthermal data. The line segments from 1 km to 24 km were derived from Star Sensor data and represent the approximate width of the weighting functions used in the data reduction. The horizontal scale is in height above the observatory which is at an altitude of approximately 10,000 ft. The tropopause height was determined from rawinsonde temperature profiles obtained from the two Hawaiian Weather Bureau stations.

For comparison, the turbulence profile used for our calculation, i.e., Eqs. (5) and (6) are given by the dashed curve in Fig. 2, along with the value of  $V$  for the date in question.

We have computed  $r_o$  based on the assumption that the plane of the receiver is 10 m above local ground and the use of Eq. (5) for high altitude turbulence and Eq. (6) for turbulence near the ground. The numerical results for  $\theta = 0$  are plotted in Fig. 3 as a function of  $V$  (upper curve). Also, we have computed the values of  $r_o$  based on Eq. (5) above and these results are also shown in Fig. 3 (lower curve). Examination of Fig. 3 reveals that for  $5 \leq V \leq 15$  m/sec the values of  $r_o$  obtained by including turbulence near the ground are within a factor of two to that obtained otherwise. For larger values of  $V$ , the corresponding values of  $r_o$  approach one another asymptotically. This is expected since for large values of  $V$  the main contribution to  $r_o$  results from turbulence values at high altitudes.

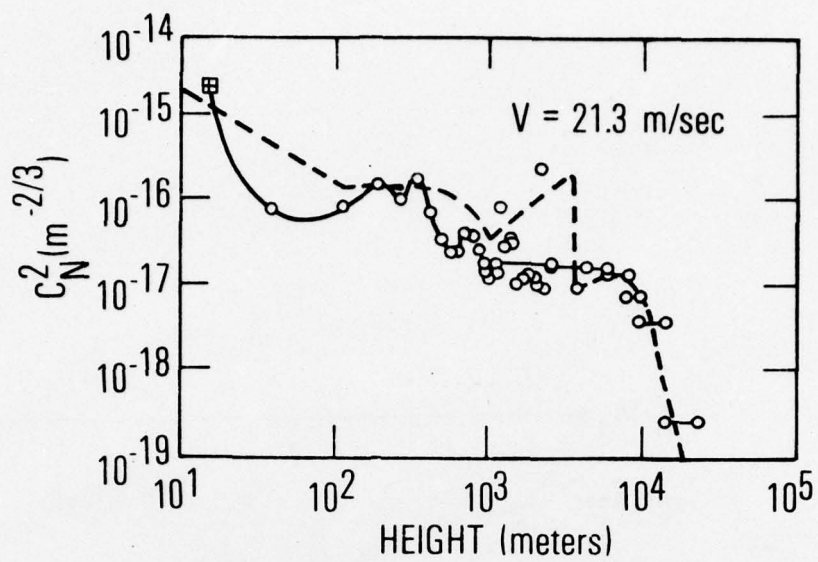


Fig. 2a. Turbulence Profile vs Height Above the Observatory - 17 November 1975.  
 Ground Based Microthermal Data =  $\square$ ;  
 Airborne Microthermal Data = +;  
 Star Sensor Data = ++. Estimated tropopause height of 11-15.5 km.  
 The dotted curve is the sum of Eqs. (5) and (6) for the value of  $V$  indicated

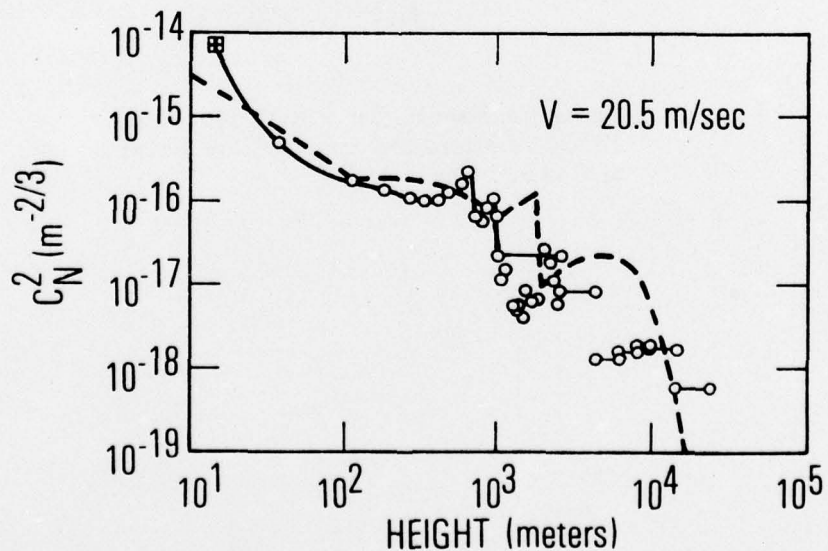


Fig. 2b. Same as Figure 2b for 18 November 1975. Estimated tropopause height of 9-15.5 km.

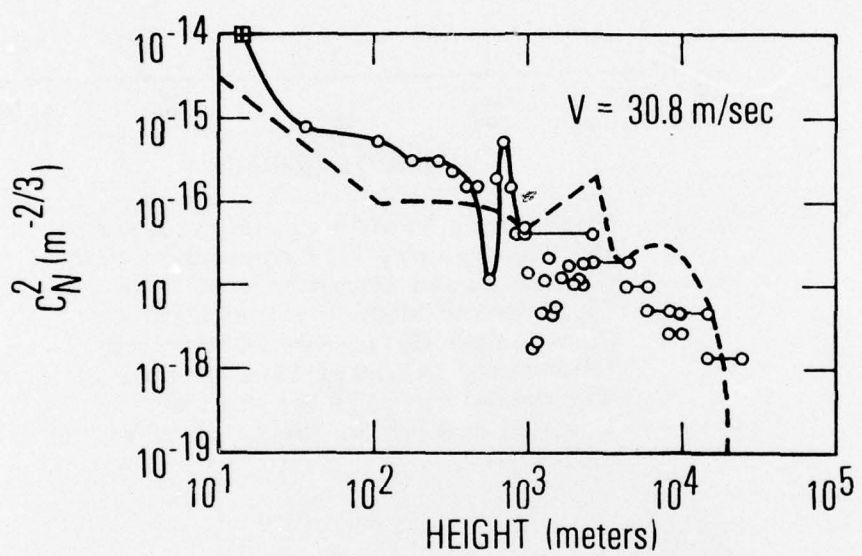


Fig. 2c. Same as Figure 2b for 21 November 1975. Estimated tropopause height of 9-15.5 km.

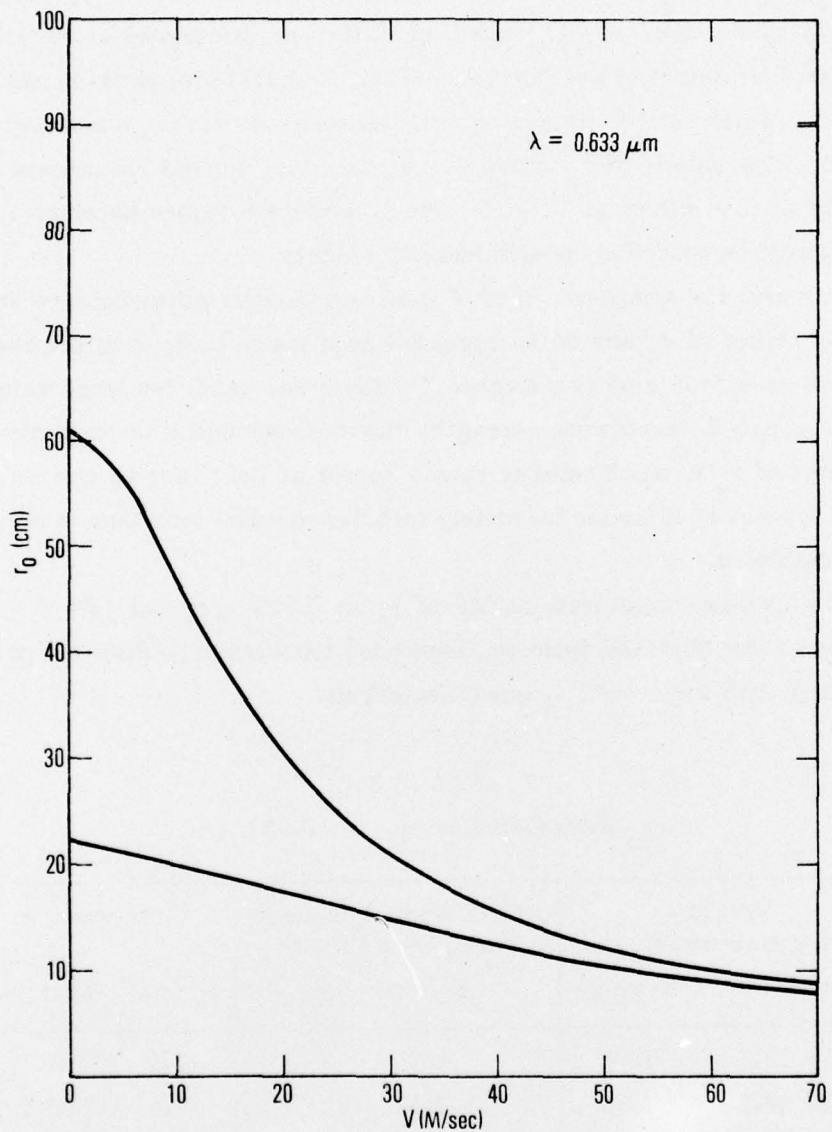


Fig. 3. The phase coherence diameter  $\lambda = 0.633 \mu\text{m}$  as function of rms wind speed. The upper curve is based on Hufnagel's model for high altitude turbulence while the lower curve includes the contribution from low altitude turbulence as given by Eq. (16).

The use of Eq. (6) for low altitude turbulence values may not be representative of the conditions above the AMOS site as it was developed from measurements made over level ground at different geographical location and averaged over different times of the year. Thus, it should represent, in our opinion somewhat of a worst case estimate of turbulence above local ground and is used here as such. The values of  $r_o$  obtained by employing Eq. (6) represents a worst case estimate at low values of  $V$  ( $\lesssim 15$  m/sec), while the values obtained for large values of  $V$  should be looked upon with less uncertainty.

In summary, for small values of  $V$  (i.e., low integrated turbulence strength) the predicted values of  $r_o$  are to be regarded as a lower limit with the real value being as much as a factor of two larger. On the other hand, for large values of  $V$  (i.e., high integrated turbulence strength) the corresponding uncertainty in the predicted value of  $r_o$  is much smaller than a factor of two; that is, the confidence by which we predict  $r_o$  is larger for strong turbulence conditions than it is for weak turbulence conditions.

AVCO's average measured values of  $r_o$  at  $0.633 \mu\text{m}$  and  $\theta = 0^\circ$  and the corresponding values obtained from the measured turbulence profiles are presented in Table 2 along with the results of our calculations.

TABLE 2  
 $r_o$  Data Comparison,  $\lambda = 0.633 \mu\text{m}$

Date	AVCO Seeing Monitor, $r_o$ (cm)		AVCO, From Measured Turbulence Profile, $r_o$ (cm)	Aerospace	
	Range	Average		$r_o$ (cm)	$V$ (m/sec)
Nov 17	9.3 - 13.5	10.4	25.7	17.1	21.3
Nov 18	13.3 - 18.2	15.4	24.9	17.4	20.5
Nov 21	9.4 - 14.4	11.8	16.6	14.4	30.8

The corresponding value of  $r_o$  at  $\lambda = 0.5$  m are obtained from those given in the table by multiplication by  $(0.5 / 0.633)^{6/5} \approx 0.75$ . Examination of Table 2 reveals that our values of  $r_o$  are in fair agreement with the experimental value. On the other hand AVCO's calculated values based on the measured turbulence profile are larger than the measured value by a factor of 1.5 - 2.

Note that for the three days considered the measured average values of  $r_o$  are somewhat less than the corresponding calculated values. At this point it is not clear why this should be the case, although it may just be an artifact. Although the airborne microthermal probe measurement of  $C_n^2$  between 37 m and 2 km above the AMOS site were performed at night, the airplane was not directly above the mountain top, but instead was slightly off to one side. This suggests that the lower altitude measured values of  $C_n^2$  probably underestimate the actual values of  $C_n^2$  directly above the AMOS site, although it is not clear that this is the case. Based on these measured values of  $C_n^2$  the AVCO calculated value of  $r_o$  is about a factor of two too large. We wait with anticipation for reliable low altitude  $C_n^2$  profile measurements above the AMOS site (i.e., from the NOAA acoustic sounder). On the other hand, we arbitrarily used a model of low altitude turbulence that, strictly speaking, applies (if at all) to conditions over level ground near sea level. For the values of  $V$  that applied, the contribution to  $r_o$  from turbulence in the first three kilometers above the site is about equal to the corresponding contribution from turbulence in the tropopause (See Fig. 2). On this basis we would expect that an  $r_o$  calculated with such a turbulence profile would result in too small a value. Since our calculated values of  $r_o$  are a little on the high side, we are left in a quandry. Rather than speculate we defer further discussions on this point until more data is analyzed.

Based on our results obtained for the three dates in question, we are encouraged to make further comparisons with more data.

In conclusion we are cautiously optimistic about the use of the model of  $C_n^2$  used here to obtain phase and log-amplitude statistics. More data comparison is clearly needed until the general use of the model can be ascertained. In particular, it is very desirable to obtain wind speed data that pertain to the time and location of the experiment. We have been in contact with P. Zieske, AVCO/Maui, and he is in process of seeing what can be done for the experiments that will be performed at AMOS this spring and summer.

REFERENCES

1. R. E. Hufnagel, "Variations of Atmospheric Turbulence," Paper WA1 appearing in the Digest of Technical Papers, Topical Meeting on Optical Propagation Through Turbulence, July 9-11, 1974, Univ. Colorado, Boulder, CO.
2. J. L. Bufton, "Comparison of Vertical Turbulence Structure with Stellar Observations," *Appl. Opt.* 12, 1785 (1973).
3. V. R. Koprof and L. R. Tsvang, "Characteristics of Very Small Scale Turbulence in a Stratified Boundary Layer," *Atmos. and Oceanic Phys.* 22, 1142 (1966).
4. V. I. Tatarskii, "Wave Propagation in a Turbulent Medium," McGraw Hill Book Co., New York (1961).
5. R. F. Lutomirski, R. E. Huschke, W. C. Meecham, and H. T. Yura, "Degradation of Laser Systems by Atmospheric Turbulence," Rand Report No. R-1171-ARPA/RC, June 1973.
6. M. Miller, P. Zieske, and D. Hanson, "Characterization of Atmospheric Turbulence," SPIE Symposium on Imaging Through the Atmosphere, Paper 7505, Reston, VA, March 1976.

PRECEDING PAGE BLANK-NOT FILMED

#### THE IVAN A. GETTING LABORATORIES

The Laboratory Operations of The Aerospace Corporation is conducting experimental and theoretical investigations necessary for the evaluation and application of scientific advances to new military concepts and systems. Versatility and flexibility have been developed to a high degree by the laboratory personnel in dealing with the many problems encountered in the nation's rapidly developing space and missile systems. Expertise in the latest scientific developments is vital to the accomplishment of tasks related to these problems. The laboratories that contribute to this research are:

Aerophysics Laboratory: Launch and reentry aerodynamics, heat transfer, reentry physics, chemical kinetics, structural mechanics, flight dynamics, atmospheric pollution, and high-power gas lasers.

Chemistry and Physics Laboratory: Atmospheric reactions and atmospheric optics, chemical reactions in polluted atmospheres, chemical reactions of excited species in rocket plumes, chemical thermodynamics, plasma and laser-induced reactions, laser chemistry, propulsion chemistry, space vacuum and radiation effects on materials, lubrication and surface phenomena, photo-sensitive materials and sensors, high precision laser ranging, and the application of physics and chemistry to problems of law enforcement and biomedicine.

Electronics Research Laboratory: Electromagnetic theory, devices, and propagation phenomena, including plasma electromagnetics; quantum electronics, lasers, and electro-optics; communication sciences, applied electronics, semiconducting, superconducting, and crystal device physics, optical and acoustical imaging; atmospheric pollution; millimeter wave and far-infrared technology.

Materials Sciences Laboratory: Development of new materials; metal matrix composites and new forms of carbon; test and evaluation of graphite and ceramics in reentry; spacecraft materials and electronic components in nuclear weapons environment; application of fracture mechanics to stress corrosion and fatigue-induced fractures in structural metals.

Space Sciences Laboratory: Atmospheric and ionospheric physics, radiation from the atmosphere, density and composition of the atmosphere, aurorae and airglow; magnetospheric physics, cosmic rays, generation and propagation of plasma waves in the magnetosphere; solar physics, studies of solar magnetic fields; space astronomy, x-ray astronomy; the effects of nuclear explosions, magnetic storms, and solar activity on the earth's atmosphere, ionosphere, and magnetosphere; the effects of optical, electromagnetic, and particulate radiations in space on space systems.

THE AEROSPACE CORPORATION  
El Segundo, California

• • •